Biomaterials. Author manuscript; available in PMC 2017 October 01.

Published in final edited form as:
Biomaterials. 2017 April ; 123: 24–38. doi:10.1016/j.biomaterials.2017.01.022.

Binding of the chemokine CXCL12α to its natural extracellular matrix ligand heparan sulfate enables myoblast adhesion and facilitates cell motility

Dhruv Thakar[1,2], **Fabien Dalonneau**[3,4], **Elisa Migliorini**[1,2], **Hugues Lortat-Jacob**[5], **Didier Boturyn**[1,2], **Corinne Albiges-Rizo**[6], **Liliane Coche-Guerente**[1,2], **Catherine Picart**[3,4,#], and **Ralf P. Richter**[1,2,7,8,#]

[1]Université Grenoble Alpes, Département de Chimie Moléculaire (DCM), Grenoble, France

[2]CNRS, DCM, Grenoble, France

[3]CNRS UMR 5628 (LMGP), Grenoble, France

[4]Grenoble Institute of Technology, Université Grenoble Alpes, LMGP, Grenoble, France

[5]Institut de Biologie Structurale, UMR 5075, Université Grenoble Alpes, CNRS, CEA, Grenoble, France

[6]Institut Albert Bonniot, Université Grenoble Alpes, INSERM, CNRS, Grenoble, France

[7]CIC biomaGUNE, San Sebastian, Spain

[8]University of Leeds, School of Biomedical Sciences and School of Physics and Astronomy, Leeds, United Kingdom

Abstract

The chemokine CXCL12α is a potent chemoattractant that guides the migration of muscle precursor cells (myoblasts) during myogenesis and muscle regeneration. To study how the molecular presentation of chemokines influences myoblast adhesion and motility, we designed multifunctional biomimetic surfaces as a tuneable signalling platform that enabled the response of myoblasts to selected extracellular cues to be studied in a well-defined environment. Using this platform, we demonstrate that CXCL12α, when presented by its natural extracellular matrix ligand heparan sulfate (HS), enables the adhesion and spreading of myoblasts and facilitates their active migration. In contrast, myoblasts also adhered and spread on CXCL12α that was quasi-irreversibly surface-bound in the absence of HS, but were essentially immotile. Moreover, co-presentation of the cyclic RGD peptide as integrin ligand along with HS-bound CXCL12α led to enhanced spreading and motility, in a way that indicates cooperation between CXCR4 (the

[#]Corresponding authors: Ralf Richter, School of Biomedical Sciences, University of Leeds, Garstang 5.55r, Leeds LS2 9JT, United Kingdom; phone: +44 113 34 31969; r.richter@leeds.ac.uk; and Catherine Picart, CNRS UMR 5628 (LMGP), Université Grenoble Alpes, 3 Parvis Louis Néel, 38016 Grenoble, France; phone: +33 4 56 52 93 11; fax: +33 4 56 52 93 01; catherine.picart@grenoble-inp.fr.

Author contributions

RPR conceived and coordinated the study; all authors contributed to designing the research and analyzing the data; DT carried out surface preparation, QCM-D and ellipsometry measurements; DT and FD performed cellular assays; DT, CP and RPR wrote the manuscript; all authors read and commented on the manuscript.

Europe PMC Funders Author Manuscripts

CXCL12α receptor) and integrins (the RGD receptors). Our findings reveal the critical role of HS in CXCL12α induced myoblast adhesion and migration. The biomimetic surfaces developed here hold promise for mechanistic studies of cellular responses to different presentations of biomolecules. They may be broadly applicable for dissecting the signalling pathways underlying receptor cross-talks, and thus may guide the development of novel biomaterials that promote highly specific cellular responses.

Keywords

Glycosaminoglycan; chemokine; cell adhesion and migration; biomimetics; bioactive surfaces; extracellular matrix

1 Introduction

Muscle development and repair are highly organized processes orchestrated by muscle progenitor cells and crucial for body function [1]: skeletal muscle stem cells (satellite cells) that are typically quiescent undergo a series of modifications including activation, proliferation and differentiation into myoblasts in response to muscle injury, and *in vitro* studies have shown that the migration of myoblasts is crucial for myogenesis and muscle regeneration [2–4]. Cell adhesion and migration are early events necessary to achieve cell–cell contacts, which are essential for the alignment of myoblasts, their subsequent fusion and formation of myotubes [2, 4–6]. Migration is a complex process that is guided by chemokines, small soluble signalling proteins that exhibit chemoattractant properties [7]. Chemokines are secreted in response to injury but they are also required for the migration of muscle precursor cells during embryogenesis [6]. In particular, the chemokine CXCL12α, previously called stromal cell-derived factor-1α, SDF-1α, and its major receptor CXCR4 have been shown to be important for the migration of myoblasts during myogenesis and muscle regeneration, both *in vivo* [6, 8–10] and *in vitro* [11–13].

Once secreted, chemokines are usually sequestered and presented to the cells *via* the extracellular matrix (ECM), notably *via* glycosaminoglycans (GAGs) such as heparan sulfate (HS) or chondroitin sulfate (CS) [14]. GAGs are linear, flexible polysaccharides and ubiquitously present at the cell surface and in the ECM. Most GAGs are covalently attached through their reducing end to core proteins, thus forming proteoglycans [15, 16]. GAGs bind to a plethora of proteins, including chemokines, and *via* these interactions, regulate matrix assembly and remodelling, as well as cell-matrix and cell-cell interactions [17]. The interaction between GAGs and chemokines is reversible and chemokines retain a certain degree of mobility in the ECM: by binding chemokines, GAGs help organizing and maintaining extracellular gradients of chemokines, thus providing directional cues for migrating cells [18–22]. Even though the functional importance of HS as an ECM ligand for chemokines is well established, the effects that the presentation of CXCL12α chemokines through HS has on the recognition of chemokines by the cells and the ensuing cellular responses such as spreading and migration has not been studied in detail.

An important requirement for myoblasts and other cells to be able to migrate is a balance between adhesion and detachment [23]. Integrins are well established as receptors for cell

Europe PMC Funders Author Manuscripts

adhesion, and known to act by binding to specific sites such as the arginylglycylaspartic acid (RGD) tripeptide present in ECM structural proteins like fibronectin and collagen. Among the members of the large integrin family, β1 and β3 integrins have been identified to be important for myogenesis *in vivo* and *in vitro* [1, 24–29]. The precise role of their involvement in myoblast adhesion and more importantly, migration, has not yet been studied. There are also several alpha integrin subunits expressed by myoblasts. Among these, α7 integrin is known to be highly expressed after myoblast fusion and associated with the maturation into myotubes [25]. This integrin subunit is thus used as a marker for primitive muscle cells although it is not expressed at the very early stage of myoblast adhesion (A. Valat, C. Picart, C. Albiges-Rizo, unpublished data). We [30] and others [31] have previously shown that the binding to integrin ligands is not strictly required for the attachment and migration of T lymphocytes, and suggested that the engagement with ECM-bound chemokines is sufficient for these processes to occur. This raises the question if myoblasts, which in contrast to T lymphocytes adhere constitutively to integrin ligands, are similarly able to migrate in chemokine-presenting environments even in the absence of integrin ligands. Ultimately, it is also important to understand how concurrent stimulation of chemokine receptors and integrins affects the balance between myoblast adhesion and detachment, and eventually, migration (haptotactic balance).

Biomimetic *in vitro* environments have emerged as important tools for studying how one or several specific extracellular cues regulate cell behaviour [29, 32–35]. Such mechanistic studies are difficult *in vivo*, because the native environment is too complex, the accessible parameter range is restricted and it is difficult to control one parameter without simultaneously affecting others. Biomimetic environments enable to dissect the role of individual parameters to cellular responses, and how a subset of defined biochemical or physical signals defines cell behaviour. In this way, they can provide insight that is difficult to obtain *in vivo*, and are complementary to *in vivo* work were cell migration is probed in the much more complex native environment. Traditionally, *in vitro* biological studies aimed at understanding the role of chemokines in physiological processes, including myogenesis, have used chemokines in a soluble form, by adding them in the cell culture medium [6, 11–13]. This is distinct from the physiological environment where chemokines are not free in solution but partly engaged in the ECM. It is only recently that an *in vitro* approach has emerged to present CXCL12α in a matrix-bound manner to myoblasts [36], using a physical entrapment of the chemokine in a biopolymeric film made by self-assembly of hyaluronan and poly(L-lysine). This study revealed that the delivery in a matrix-bound fashion potentiates the effect of CXCL12α in cellular processes of relevance for myogenesis, such as myoblast adhesion and motility, compared to soluble CXCL12α. Several questions remain unanswered, however, that are of importance for the fundamental understanding of myoblast guidance by extracellular cues and also of interest for the rational design of new functional biomaterials. Firstly, is the mode of chemokine entrapment irrelevant, or would a presentation of CXCL12α, for example through HS as its native matrix ligand, elicit different effects? Secondly, how do integrin ligands modulate the response of myoblasts to matrix-bound CXCL12α? Being able to control precisely the orientation and presentation mode of chemokine (*via* GAGs) as well as to present other active molecules able to target adhesion receptors would enable to study the importance of the presentation mode of the

chemokine, and to investigate the interplay of matrix-bound chemokines and integrin ligands in guiding the cellular behaviour.

To this end, the biofunctionalization of solid surfaces is an attractive route [37–41]. We have recently presented a ‘molecular breadboard’ technology for the formation of multifunctional biomimetic surfaces that reproduce selected features of extracellular matrix [30] (Fig. 1A). The technology enables the design of surfaces that co-present several desired biomolecules, each at controlled orientation (and thus functionality) and at tuneable density, in a background that suppresses non-specific binding. In contrast to conventional cellular studies where molecules are either being randomly immobilised or added to the solution, and where cells may adhere non-specifically, these surfaces are useful as tuneable signalling platforms that present defined sets of desired extracellular cues without interference from other matrix signals.

In the present study, we focus our attention on muscle extracellular matrix and two bioactive cues, the CXCL12α chemokine and the cyclic RGD (cRGD) integrin ligand, in myoblast adhesion and motility. Our main objectives were to probe if the mode of chemokine presentation is important for myoblast behaviour, and how the chemokine and the integrin ligand jointly affect myoblasts as compared to their individual effects. For this purpose, we engineered biomimetic surfaces that (i) present CXCL12α in two distinct ways (either through their native matrix ligand HS or directly immobilized), (ii) reproduce the supramolecular arrangement of extracellular GAGs (with HS being attached to the surface through the reducing end, thus mimicking the native attachment of HS to its proteoglycan core), and (iii) present cRGD (known to adhere most potently to β_3 integrins and to a lesser extent to β_1 or other integrins [42, 43]). In this first study with this platform, we focus on the myoblast phenotype such as adhesion, spreading, motility and cytoskeletal organization, and demonstrate how mechanistic studies on early stages of *in vitro* muscle regeneration are enabled by an environment that is well-defined and tuneable. Specifically, we reveal that the presentation of CXCL12α through HS facilitates myoblast migration when compared to CXCL12α alone, that CXCL12α as the only extrinsic signal is sufficient for active cell migration, and that cRGD potentiates the spreading and motility induced by CXCL12α. The results demonstrate that the mode of CXCL12α presentation is crucial to the adhesion and migration of myoblasts.

2 Materials and methods

2.1 Buffer, heparan sulfate, proteins and other molecular building blocks

The working buffer used for all experiments and for protein dilution was made of 10 mM Hepes at pH 7.4 (Fisher, Illkirch, France) and 150 mM NaCl (Sigma Aldrich, Saint-Quentin Fallavier, France) in ultrapure water. Heparan sulfate (HS) derived from porcine intestinal mucosa with an average molecular weight of 12 kDa and a polydispersity of 1.6 (Celsus Laboratories, Cincinnati, OH, USA) was conjugated with biotin, site-specifically attached to the reducing end by oxime ligation [44]. Recombinant CXCL12α (amino acids 1 to 68; 8.1 kDa) was prepared as previously reported [45]. The same protein with a biotin conjugated to the C-terminal lysine through a tetraethylene glycol linker (b-CXCL12α; 8.6 kDa) was produced by solid-phase peptide synthesis as previously reported [46]. Lyophilized

streptavidin (60 kDa) and bovine serum albumin (BSA) were purchased from Sigma Aldrich. All proteins were diluted to 0.2 mg/mL in autoclaved working buffer and stored at -20°C. Thawed protein solutions were used within 5 days and further diluted as desired. Polyethylene glycol (PEG, 3.2 kDa) with a biotin at one end and an OH group at the other (b-PEG) was purchased from Iris Biotech (France). b-cRGD (3.9 kDa) was obtained by amide-coupling of linear PEG (3.2 kDa) with a biotin at one end and an activated acid group at the other end (b-PEG-NHS; Iris Biotech) to a RGD-containing cyclic pentapeptide c(-RGD*f*K-) at the lysine side-chain as described previously [47].

2.2 Surfaces and surface functionalization

Quartz crystal microbalance with dissipation monitoring (QCM-D) sensors with gold coating (QSX301) were purchased from Biolin Scientific (Västra Frölunda, Sweden). Appropriately sized wafers with an optically opaque gold coating (100 nm, sputter-coated) were used for SE measurements. Glass cover slips (24 × 24 mm^2; Menzel Gläser, Braunschweig, Germany) with a semi-transparent gold film (~5 nm) were prepared, as described previously [30]. To create a biotin-displaying and otherwise inert background, the gold-coated surfaces were conditioned with UV/ozone (Jelight, Irvine, CA, USA) for 10 min and then immersed overnight in an ethanolic solution (Fisher) of oligo ethylene glycol (OEG) disulfide (containing 7 EG units per arm) and biotinylated OEG thiol (containing 10 EG units; both Polypure, Oslo, Norway) at a total concentration of 1 mM and a molar ratio of thiol equivalents of 999:1.

2.3 Assembly of biomimetic surface coatings

A monolayer of streptavidin on a gold-supported biotinylated OEG monolayer (Fig. 1A) served as a ‘molecular breadboard’ onto which the desired molecules were sequentially assembled. To prepare chemokine-presenting surfaces (Fig. 1B), the following concentrations and exposure times were used: b-HS - 50 μg/mL, 30 min; CXCL12α – 5 μg/mL (620 nM), 30 min; b-CXCL12α – 5 μg/mL (580 nM), 30 min. Under these conditions, binding is expected to saturate or equilibrate, irrespective of whether the solution is flown (in QCM-D measurements), or still (in spectroscopic ellipsometry (SE) measurements and for cell assays). To prepare multifunctional surfaces (Fig. 4), the following concentrations and incubation times were used: b-HS - 1 μg/mL, 30 min; b-cRGD - 1 μg/mL, 5 min (Fig. 4A-C) or 90 s (Fig. 4D); b-PEG - 50 μg/mL, 20 min; CXCL12α – 5 μg/mL (620 nM), 30 min. Here, the reduced concentrations and/or incubation times of HS and cRGD were chosen to obtain the desired sub-monolayer surface densities (Fig. 4 and Table 2); b-PEG was incubated to back-fill the remaining biotin-binding pockets on the streptavidin monolayer, and eventually CXCL12α was incubated until equilibrium where desired.

2.4 Quartz crystal microbalance with dissipation monitoring (QCM-D)

QCM-D was used to ascertain that the desired functionalities can be realized with controlled orientation, as it provides time-resolved information about the assembly process, including the overall morphology and mechanical properties of the biomimetic film [48]. QCM-D measures the changes in resonance frequency, Δf, and dissipation, ΔD, of a sensor crystal upon molecular adsorption on its surface. The QCM-D response is sensitive to the mass

(including hydrodynamically coupled water) and the mechanical properties of the surface-bound layer. Measurements were performed with a Q-Sense E4 system equipped with four independent Flow Modules (Biolin Scientific) and gold-coated QCM-D sensors functionalized with biotinylated OEG monolayers. The system was operated in flow mode with a flow rate of typically 10 μL/min, at a working temperature of 24 °C. Δf and ΔD were measured at six overtones (i = 3, 5, …, 13), corresponding to resonance frequencies of $f_i \approx$ 15, 25, …, 65 MHz; changes in dissipation and normalized frequency, $\Delta f = \Delta f_i/i$, of the third overtone (i = 3) are presented; any other overtone would have provided comparable information.

2.5 Spectroscopic ellipsometry (SE)

SE measures changes in the polarization of light upon reflection at a planar surface. SE was employed in aqueous environment with a M2000V system (J. A. Woollam, Lincoln, NE, USA) to quantify the surface density of adsorbed biomolecules in a time-resolved manner. Gold-coated silica wafers functionalized with biotinylated OEG monolayers were installed in a custom-built open cuvette (~120 μL) featuring a magnetic stirrer for homogenization of the cuvette content (typically for 5 s after pipetting a sample into the solution) and a flow-through system for rapid solution exchange during rinsing steps. Before use, the cuvette walls were passivated against biomolecular binding by exposure to a 10 mg/mL BSA solution in working buffer (20 min), followed by rinsing with ultrapure water and blow-drying with N_2 gas. Biomolecular binding processes were monitored at room temperature. Surface densities were quantified through fitting of the data to optical models, as described in detail elsewhere [49]. Briefly, the opaque gold film and the OEG monolayer were treated as a single isotropic layer and fitted as a B-spline substrate. Areal mass densities were determined through de Fejter's equation, using refractive index increments, dn/dc, of 0.132 cm^3/g for b-HS [50–52], 0.18 cm^3/g for all proteins [53, 54], 0.15 cm^3/g for b-cRGD (estimated from the dn/dc of the individual amino acids and the PEG chain using an established method [54–56]), and 0.134 cm^3/g for b-PEG [57]. All measurements were repeated twice and the data represent mean ± standard errors.

2.6 Cell culture

The mouse myoblast cell line C2C12 (<20 passages post-delivery from American Type Culture Collection (ATCC)) was cultured as previously described [58]. Briefly, cells were grown at low cell density in a medium containing 10% serum. Under these conditions, the fusion of cells is avoided, which would occur at high cell density in low serum-containing medium (see ref. [28] for details). Prior to the cell assays, serum was removed from the cell suspension, by centrifugation at 600 rpm at 25 °C for 10 min; the supernatant was then removed and the cells were exposed to serum-free 1:1 DMEM/F12 medium (Life Technology, Saint-Aubin, France). Cell adhesion assays were performed with custom-made 4-well plates with ~100 μl solution per well and a functionalized glass cover slip on the bottom, prepared as described previously [30]. Surfaces with the desired biomimetic coating were prepared as described above sterilized for 15 min under UV light, and C2C12 cells were seeded at a density of 1.5×10^4 cells/cm^2 by adding 90 μL of cell suspension to 10 μL of working buffer (either pure or with 5 μg/mL CXCL12α). CXCL12α binds reversibly to HS and thus partitions between the HS-coated surface and the solution; based on the

conditions employed for liquid exchange and cell seeding, we estimate the residual CXCL12α concentration in solution to be around 0.5 μg/mL (60 nM). After incubation for 1 h and 4 h, non-adhesive (and weakly adhesive) cells were removed by gentle rinsing with sterile phosphate-buffered saline (PBS, pH 7.4; Sigma Aldrich) using a pipette. To test for the specificity of the cellular recognition of CXCL12α through the receptor CXCR4, the cell suspension was supplemented with the CXCR4 antagonist AMD3100 (Sigma-Aldrich) at a concentration of 50 μM, which inhibits interaction of CXCR4 with CXCL12α [6, 11]. To test whether integrins are associated with CXCL12α mediated adhesion, the cell suspension was supplemented with soluble cRGD at a concentration of 2 mM, which blocks/saturates the $\alpha_v\beta_3$ and $\alpha_5\beta_1$ integrins [59–61]. All cell assays were repeated 3 times.

2.7 Quantitative analysis of cell adhesion, cell spreading and cell morphology

For quantification of cell adhesion, 10 bright-field images of cells per sample were recorded shortly before and after gentle rinsing using an inverted microscope (Axiovert 200 M; Carl Zeiss SAS, Le Pecq, France) equipped with a 10× objective, covering a surface area of at least 2 mm^2 in total. The number of surface-proximal cells was counted manually. The percentage of adherent cells was defined as the ratio between the number of cells after rinsing and before rinsing.

For quantitative analysis of cell spreading and morphology, adhered cells were first rinsed in phosphate-buffered saline (PBS, Sigma-Aldrich) and fixed with 3.7% formaldehyde (Sigma-Aldrich) in PBS for 20 min before being incubated overnight in 0.5% BSA in PBS at 4°C. The cells were then permeabilized in 0.2% Triton X-100 in Tris-buffered saline (TBS; 50 mM Tris, 150 mM NaCl, 0.1% NaN_3, pH 7.4) for 4 min, incubated with rhodamine-phalloidin (Sigma-Aldrich; 1:800 in 0.2% gelatin (Sigma-Aldrich) in TBS) for labelling actin and with DAPI (Sigma-Aldrich; 1:100 in 0.2% gelatin in TBS) for labeling the nucleus, and then imaged with an Axiovert 200 M epi-fluorescence microscope or an LSM 700 confocal microscope (both Carl Zeiss SAS) using a 20× objective. To quantify cell spreading and circularity, fluorescence images were analyzed with ImageJ software by marking the cellular perimeter (as defined by the actin labeling) manually, to determine the projected area and circularity of the cells. Circularity is defined as $4\pi(\text{area}/\text{perimeter}^2)$, *i.e.* a circularity of 1 corresponds to a cell with a circular projected area and a value close to 0 to a cell with a very high perimeter.

The major cell adhesion receptors in C2C12 myoblasts, β_1 and β_3 integrins [27], were also stained. The cells were first fixed, blocked in 0.5% BSA in PBS, permeabilized in 0.2% Triton X-100 in TBS, and integrins were then immuno-stained with anti-β_1 MB1.2 (1:100; Merck Millipore; Alsace, France) and anti-β_3 Luc.A5 (1:100; Emfret Analytics, Wurzburg, Germany) monoclonal antibodies and AlexaFluor488-conjugated secondary antibody (1:100; Life Technology).

2.8 Quantification of cell migration

To assess the motility of cells, these were imaged every 5 min for 4 h after seeding on biomimetic surfaces, using an LSM 700 confocal microscope equipped with a 5× objective and an environmental chamber (providing 37 °C and 5% CO_2). Time-lapse image series

were assembled and analyzed using ImageJ software. Individual cell tracking was performed using the "Manual tracking" plugin, which allows selecting a cell and recording its movement by following the cell position across the image frames. The motion traces were then displayed and statistically analyzed using the "Chemotaxis tool".

2.9 Data and statistical analysis

Data on cell adhesion represent the mean and standard deviation (S.D.) over the percentage of adherent cells across three independent experiments with typically 500 cells per sample. Data showing cell area, circularity and cell migration are represented as box plots, the small square and the horizontal line inside the box indicating the mean and the median, respectively, the box delimiting the 25% to 75% percentile of data, and the error bar representing the lower 10% and 90% limits, respectively. Here, a total of 120 cells, *i.e.* 3 independent experiments with 40 cells were analyzed per sample. For motility assays, the mean velocity was computed over intervals of 0.5 h and data represent the average and standard errors of the mean (S.E.M.); 80 cells were tracked per sample and experiments were repeated thrice.

Statistical comparisons were performed using Origin 8.1 software. When comparing data between more than two groups, analysis of variance (ANOVA) followed by an appropriate pair wise comparison or comparison versus control group was performed to obtain p-values (lines with an asterisk indicate $p < 0.05$; dotted lines indicate no significant difference).

3 Results

To study the response of myoblasts towards the mode of chemokine CXCL12α presentation, our approach consisted in designing tailor-made biomimetic model surfaces encompassing CXCL12α, the GAG HS and the integrin ligand cRGD with controlled orientation and at tuneable densities. A monolayer of streptavidin on a gold-supported biotinylated OEG monolayer served as a 'molecular breadboard' onto which the desired molecules were sequentially assembled in a background of low non-specific binding [30] (Fig. 1A). Before construction of multifunctional surfaces, we ascertained that the desired functionalities can be realized with controlled orientation. For this purpose, QCM-D was used, providing time-resolved information about the assembly process, including overall film morphology and mechanical properties. Figure S1 shows that all the constituents of the biomimetic surfaces can be attached to surfaces in a specific way through site-specifically conjugated biotins for b-HS, b-CXCL12α and b-cRGD, and through biospecific binding to HS for CXCL12α [62]. Thus, their presentation can be precisely controlled. To facilitate the reader's orientation, we have listed in Table 1 all prefixes used to indicate the various modes of presentation, and particular molecular properties and tags, of the functional molecules employed throughout this study.

3.1 Preparation of well-defined biomimetic surfaces with distinct CXCL12α presentations

In a first step, we designed surfaces presenting CXCL12α in two distinct ways: either *via* reversible adsorption to its native matrix ligand heparan sulfate (*i*HS + *a*CXCl12α) or directly immobilized on the surface (*i*CXCL12α) (Fig. 1B, left). In these conditions, the

molecule of interest is either reversibly adsorbed ("*a*") or quasi-irreversibly immobilized ("*i*"). Spectroscopic ellipsometry was used to quantify the surface densities of biomolecules during the step-by-step assembly process (Fig. 1, right). Table 2 summarizes the adsorbed amounts and lateral root-mean-square (rms) distances for the constituents of the biomimetic surfaces.

Sample incubations in the spectroscopic ellipsometry measurements were performed in still solution, *i.e.* under mass-transport conditions that were identical to those subsequently used for the preparation of surfaces for cellular assays. The areal mass density for the streptavidin monolayer was 235 ± 5 ng/cm^2, reproducing previous work [30]. To immobilize HS (*i*HS), b-HS was incubated to saturation and the corresponding areal mass density was 40 ± 2 ng/cm^2. This would correspond to a root-mean-square distance of 7 nm between HS anchor points on the surface, if we assume that the mean molecular weight of the surface-bound HS is 12 kDa, *i.e.* identical to the mean molecular weight of HS in the incubation solution. In reality, small-sized HS is likely to bind preferentially and the average size of the surface-bound HS is thus likely to be smaller (see ref. [30] for details). Assuming that each streptavidin molecule displays two of its four biotin binding sites to the solution (with the other two being used for immobilization on the surface) and that two HS chains bind per streptavidin at maximal coverage, we obtain a root-mean-square anchor distance of 5 nm and a mean molecular weight of 4.6 kDa. The values of 5 nm and 7 nm thus represent lower and upper boundaries of the real anchor distance. Subsequent incubation of CXCL12α (*i*HS + *a*CXCL12α) at 5 μg/mL led to an adsorbed surface density of 78 ± 7 ng/cm^2, or a mean lateral distance of 4 nm. To immobilize CXCL12α (*i*CXCL12α), biotinylated CXCL12α was incubated to full coverage, corresponding to 60 ± 1 ng/cm^2 or a mean distance of 5 nm. The biotin being located site-specifically at the C-terminal residue, it is not expected to interfere with CXCL12α binding to the cell surface receptor CXCR4 [30, 63]. We note that HS is known to induce the formation of CXCL12α dimers [62, 64, 65], and this is reflected in the sketches in Fig. 1B. Finally, the CXCL12α surface densities for the two different scenarios with *i*HS + *a*CXCL12 (78 ± 7 ng/cm^2) and *i*CXCL12α (60 ± 1 ng/cm^2) are comparable.

3.2 CXCL12α promotes C2C12 myoblast adhesion and spreading, and this depends on the mode of CXCL12α presentation

Next, we used these surfaces to evaluate how the presentation of CXCL12α impacts the adhesive behaviour of C2C12 cells, by comparing reversibly HS-bound chemokine with quasi-irreversibly immobilized chemokine. We first investigated the effects of HS-bound CXCL12α on the adhesion and spreading of C2C12 cells (Figs. 2 and S2) by bright field imaging (Figs. 2A, F and S2A) and fluorescence staining (Figs. 2B, G and S2B). The fraction of cells that resisted gentle rinsing was quantified (Fig. 2C and H), as well as the spreading (Fig. 2D and I) and circularity (Fig. 2E and J) of the adhered cells after 1 h and 4 h of contact with the surfaces. Approximately 50% of the cells on surfaces presenting exclusively *i*HS were readily removed by gentle rinsing (Fig. 2C) and the remaining cells retained a rounded phenotype irrespective of the incubation time. This indicates that the *i*HS surface is only weakly adhesive, and does not promote cell spreading. When chemokines were included (*i*HS + *a*CXCL12α), on the other hand, cells adhered strongly and spread

slowly, that is, spreading was pronounced after 4 h but not significant after 1 h of exposure (Fig. 2C-E). When CXCL12α binding to the cell-surface receptor CXCR4 was blocked with the soluble CXCR4 antagonist AMD3100 (*s*AMD3100), the fraction of adhered cells, the cell area and the circularity returned to the levels of HS alone (Fig. 2C-E). This demonstrates that the adhesion of C2C12 myoblasts to surfaces presenting HS-bound CXCL12α is mediated by the specific binding of the CXCL12α ligand to the CXCR4 receptor. Besides CXCR4, CXCR7 has been reported as another CXCL12α receptor in C2C12 myoblasts [13, 66]. Under the culture conditions used in our assays, however, CXCR7 is not expressed [36] and the AMD3100 control thus confirms CXCR4 as the major receptor.

Our results clearly show that *a*CXCL12α enables C2C12 myoblasts to adhere and spread, a cellular response that is commonly mediated by cell adhesion receptors [67–69]. For myoblasts, the established major cell adhesion receptors are $\alpha_v\beta_3$ and $\alpha_5\beta_1$ integrins [27, 28], yet by their design the here-employed surfaces did not present integrin ligands. The C2C12 cells may secrete matrix molecules such as fibronectin to which integrins could bind. However, adding the integrin ligand cRGD [43] in solution (*s*cRGD) at a high concentration as a competitor did not affect the cell adhesion and spreading on *a*CXCL12α, apart from a minor increase in cell circularity (Fig. S4). Our results thus demonstrate that cell adhesion and spreading can be mediated by HS-bound CXCL12α, even in the absence of integrin-mediated initial binding.

In comparison, when cells were exposed to CXCL12α immobilized quasi-irreversibly (*i*CXCL12α) in the absence of HS, they responded strongly to the chemokine already as soon as 1 h after the start of exposure (Fig. 2H-J): cell adhesion and spreading increased while circularity was reduced compared to the bare breadboard. Prolonged exposure did not enhance spreading and circularity further (Fig. 2I-J), but the maximal level of spreading was higher than for *i*HS + *a*CXCL12α over the 4 h period (Fig. 2D). Moreover, the presence of CXCL12α added in solution (*s*CXCL12α) did not enhance cell adhesion to a bare breadboard (Fig. S3A-C), and a significant decrease in adhesion and spreading of cells on *i*CXCL12α was observed with *s*AMD3100 (Fig. 2H-J). This indicates that the adhesive response required immobilized CXCL12α and was, at least in part, mediated by CXCR4. The residual binding on *i*CXCL12α, not observed on *i*HS + *a*CXCL12α, could be due to the interaction of *i*CXCL12α with HS proteoglycans on the myoblast surface. As for *a*CXCL12α, *s*cRGD did not affect the cell adhesion and spreading on *i*CXCL12α, demonstrating that integrin-mediated initial binding is also not required for cells to adhere and spread on *i*CXCL12α.

Interestingly, the adhered cells on *i*CXCL12α showed finger-like protrusions, which appeared to mature over time (compare Figs. 2G and S2B), while no such protrusions were observed on surfaces with HS-bound *a*CXCL12α (Figs. 2B and S2B). The protrusions were enriched in actin and typically also enlarged at their ends, features that are reminiscent of filopodia with nascent adhesion sites (cf. Fig 1B in ref. [70]). The differences in both the temporal response and cell morphology demonstrate that the mode of CXCL12α presentation plays an important role in myoblast adhesion and spreading. Apparently,

distinct mechanisms are involved in chemokine recognition and downstream intracellular signalling.

3.3 The mode of CXLC12α presentation also affects cell motility

Apart from adhesion, CXCL12α also plays a key role in the migration of both proliferative and terminally differentiated muscle cells [6, 9, 71], and we asked if the differences in adhesion have functional significance for cell motility. The motility of C2C12 myoblasts was assessed by recording time-lapse images over 4 h and tracking individual cells (Fig. 3). Figure 3A-B demonstrates that the cells are essentially immotile on *i*HS alone as cells migrated within a small area and the mean velocity was low. A significant increase in the mean velocity was observed when CXCL12α was co-presented through HS (*i*HS + *a*CXCL12α). In striking contrast, such an increase was not observed on *i*CXCL12α. Fig. 3C provides insight into temporal variations in the cellular motility. Cells responded to HS-bound CXCL12α (as compared to *i*HS alone or to *i*CXCL12α) already within the first 30 min after exposure, yet about 2 h were required to reach the maximal response. The maximal response was then largely retained for the remainder of the exposure. These results, in combination with the results from cell adhesion, suggest that the presentation of CXCL12 via HS produces weaker adhesion which facilitate myoblast motility.

3.4 Preparation of multifunctional surfaces presenting CXCL12α and cRGD

Next, we aimed at investigating how C2C12 cells respond to the presentation of immobilized integrin ligands along with chemokines. In this part, we focused on the presentation of CXCL12α through a GAG as the native ECM ligand. For this purpose, we designed biomimetic surfaces that present HS-bound CXCL12α together with cRGD immobilized through a biotin to the breadboard (*i*HS + *a*CXCL12α + *i*cRGD, Fig. 4A). The streptavidin-monolayer molecular breadboard can readily accommodate multiple biotinylated compounds, generating multifunctional surfaces. Advantageously, the surface density of each compound can be tuned by adjusting its incubation conditions [30]. Here, the functional molecules of interest were presented at lower density ("*ld*") (Table 2) compared to the previous assays where they were functionalized to saturation (Fig. 1). To form the desired co-funtionalized surfaces (Fig. 4A), b-HS was first incubated with reduced concentration and for a controlled time (see Materials and methods for details) to reach a surface coverage of 15 ± 1 ng/cm^2, corresponding to a root-mean-square anchor distance between 7 and 12 nm (following the rationale outlined above). This was followed by b-cRGD incubation with conditions adjusted to obtain an areal mass density of 9 ± 2 ng/cm^2, which corresponds to a mean distance between 7 and 9 nm. b-PEG was then incubated to back-fill the remaining free biotin-binding pockets on the streptavidin breadboard. Onto this multifunctional surface, CXCL12α bound with an equilibrium surface density of 37 ± 3 ng/cm^2, or a mean distance of 6 nm. As controls, we prepared surfaces that lacked one or two of the biofunctional components (*i.e.* HS, CXCL12α, or cRGD) with the surface density of all remaining biofunctional components unchanged (Fig. 4B-D) and vacant biotin-binding sites back-filled by b-PEG. SE analysis demonstrates that comparable surface densities of *ld-i*HS and *ld-i*cRGD could indeed be obtained (Fig. 4B-D and Table 2), straightforwardly for *ld-i*HS (Fig. 4B) and *ld-i*HS + *ld-i*cRGD (Fig. 4C), and through a further modification of incubation conditions (*i.e.* a reduction in incubation time to 1.5 min) for *ld-i*cRGD (Fig. 4D,

dotted lines). The surface density of *ld-a*CXCL12α on a sub-monolayer of *ld-i*HS without *ld-i*cRGD was around 30 ng/cm^2 at equilibrium (Fig. 4B), comparable to the values observed in the presence of *ld-i*cRGD.

Thus, these multifunctional biomimetic surfaces permit presentation of chemokines and integrin ligands either alone or together, at controlled surface densities. The incubation conditions established in Fig. 4 were subsequently used for the construction of biomimetic surfaces for the cellular assays.

3.5 cRGD potentiates CXCL12α-mediated C2C12 myoblast spreading

We analyzed cell adhesion to the multifunctional surfaces (Figs. 5 and S5) in the same way as before for the cRGD-free surfaces. As a control, we first verified that the surface presenting *i*HS and *a*CXCL12α at lower densities (reduced by roughly 3-fold for *ld-i*HS and 2-fold for *ld-a*CXCL12α compared to *i*HS and *a*CXCL12α in Fig. 2, respectively; see Table 2) affected the cellular responses only slightly in the absence of cRGD. In contrast, cells adhered and spread significantly on surfaces presenting cRGD, either alone (*ld-i*cRGD) or along with HS (*ld-i*HS + *ld-i*cRGD). The cells formed pronounced actin-rich stress fibers (Fig. 5B) as expected for integrin-mediated cellular adhesion [72, 73]. Interestingly when the cells were exposed to surfaces co-presenting HS-bound CXCL12α and cRGD (*ld-i*HS + *ld-a*CXCL12α + *ld-i*cRGD), there was a significant increase in cell spreading in comparison to each stimulus (*ld-i*cRGD or *ld-a*CXCL12α) taken separately. It is particularly interesting that the combined presentation of HS-bound CXCL12α and cRGD enhanced cell spreading already after 1 h of exposure, *i.e.* under conditions at which HS-bound CXCL12α alone did not have any appreciable effect. This suggests that the enhanced spreading is a cooperative effect, that is, the co-presentation of the integrin ligand and the HS-bound chemokine elicits an adhesive response that is distinct from the response to each individual cue alone, and more than a simple superposition of the two responses.

Control measurements showed that, when cRGD was presented with HS in the absence of *a*CXCL12α (condition *ld-i*HS + *ld-i*cRGD), cellular spreading was similar to the *ld-i*cRGD condition alone (Fig. 5D). Furthermore, when CXCL12α binding to its cell-surface receptor CXCR4 was blocked with *s*AMD3100 (in the *ld-i*HS + *ld-a*CXCL12α + *ld-i*RGD condition), cell spreading was reduced to the levels observed for cRGD (*ld-i*cRGD) alone (Fig. 5D). Finally, the presence of *s*CXCL12α with *ld-i*cRGD did not enhance cell spreading (Fig. S3E). All together, these results demonstrate that the cooperative effect observed on surfaces co-presenting HS-bound CXCL12α and cRGD requires (i) the presence of HS-bound CXCL12α (*s*CXCL12α is not sufficient) and (ii) binding of CXCL12α to its receptor CXCR4.

3.6 Integrins organize differentially in response to CXCL12α vs cRGD mediated cell adhesion and spreading

To obtain insights into the expression and spatial organization of integrins in response to the interaction with our biomimetic surfaces, we performed integrin labelling (Fig. 6). We focused on β_1 and β_3 integrins, because these are known to be the major integrins involved in myoblast adhesion to extracellular matrix proteins and RGD ligands [27, 28].

Immunofluorescence staining of cells plated on *i*cRGD, and on *ld*-*i*cRGD with *ld*-*i*HS, revealed that both β_1 and β_3 integrins were present but with distinct spatial organizations: β_3 integrins showed a pronounced punctate pattern and preferential localization at the end of stress fibres that characterize focal adhesions [73–75], whereas β_1 integrins exhibited a more diffuse distribution with clusters also being present although less well defined (Fig. 6A-B). This indicates that the cells responded to immobilized cRGD primarily *via* the β_3 integrin rather than the β_1 integrin, as expected for the cyclic peptide [42].

On HS-bound CXCL12α (*i*HS + *a*CXCL12α), cells were devoid of stress fibres but actin was concentrated at the cell extremities. β_1 and β_3 integrins distributed very diffusely, were enriched at the cell extremities but did not form focal adhesions (Fig. 6C). When the cells were instead plated on immobilized chemokine (*i*CXCL12α), the two integrin patterns were again distinct: β_1 integrins and actin were strongly enriched in the filopodia-type cell protrusions, whereas β_3 integrins were quite homogeneously distributed across the cell and accumulated to a lesser extent in the protrusions (Fig. 6D).

The lack of sensitivity to *s*cRGD (Fig. S4), and the absence of focal adhesions, suggest that the integrin enrichment is not directly driven by ligands from the outside but instead results from intracellular processes downstream the activation of the CXCR4 receptor. Moreover, the clear differences in the distribution of β3 integrins suggest that the mode of CXCL12α presentation differentially affects integrin reorganization downstream CXCR4 activation. It is also noteworthy that distinct integrins responded preferentially to *i*cRGD (β_3) and *i*CXCL12α (β_1), whereas the response to *a*CXCL12α was less selective.

When the cells were presented simultaneously to HS-bound CXCL12α and to immobilized cRGD (*ld*-*i*HS + *ld*-*a*CXCL12α + *ld*-*i*cRGD), however, the spatial organization of actin and integrins was similar to *i*cRGD alone, with pronounced focal adhesions rich in β_3 integrins connecting to stress fibres, and a more diffuse distribution of β_1 integrin (although some smaller clusters can be observed, which perhaps are nascent adhesions or focal complexes [76]) (Fig. 6A and E). Apparently, *i*cRGD remains the major driver of integrin re-organization even in the presence of *a*CXCL12α.

3.7 Effect of aCXLC12α, icRGD, and their combination on cell migration

Next, we investigated if the co-presentation of the integrin ligand cRGD with HS-bound CXCL12α affected cell migration. For this purpose, we performed motility assays on multi-functional surfaces presenting HS-bound CXCL12α (*ld*-*i*HS + *ld*-*a*CXCL12α) jointly with *ld*-*i*cRGD. Figure 7 demonstrates that cell motility is retained but lower on surfaces that present a reduced density of HS-bound CXCL12α compared to HS-saturated surfaces (Fig. 3). Cells were essentially immotile on surfaces presenting *ld*-*i*cRGD irrespective of the presence of *ld*-*i*HS. Remarkably, HS-bound CXCL12α in combination with cRGD (*ld*-*i*HS + *ld*-*a*CXCL12α + *ld*-*i*cRGD) promoted a level of motility that was higher than that observed for HS-bound CXCL12α alone. Notably, the mean velocity of the cells on HS-bound CXCL12α in the presence of cRGD rose to a maximum within the first 1.5 h, and then decreased again (Fig. 7C). This is in contrast to HS-bound CXCL12α alone, where motility reached a plateau value (Fig. 3C and 7C). Together with the results on adhesion, these data

show that HS-bound CXCL12α and cRGD exert cooperative effects on cell spreading as well as motility.

4 Discussion

We have developed a methodological approach to prepare well-defined biomimetic environments that mimic selected aspects of muscle extracellular matrix and demonstrated their application as a tuneable signalling platform for quantitative cellular studies. Our results shed light on the important role of HS as extracellular ligand of the chemokine CXCL12α, and the cooperative effect of CXCL12α and the integrin ligand cRGD, on basic features of the myoblast phenotype in response to CXCL12α – adhesion, spreading, motility and cytoskeletal (integrin and actin) organization – that are of importance in the very early steps of myogenesis. In the following, we recapitulate the main findings and discuss possible molecular mechanisms.

The presentation of CXCL12α through heparan sulfate enables myoblast adhesion and facilitates cell migration

Previous work [36] had already revealed that matrix-bound CXCL12α can elicit cellular processes in a serum-containing medium over the time course of 24 h that soluble CXCL12α is unable to trigger. A major finding of the present study is that the mode of CXCL12α presentation by the substrate is also a crucial regulator of myoblast adhesion and migration. Specifically, although both *a*CXCL12α and *i*CXCL12α clearly permitted engagement with the CXCR4 receptor and thus enabled C2C12 myoblast adhesion and spreading (Fig. 2), the presentation of CXCL12α through HS was required to facilitate cell motility (Fig. 3). We may propose several hypotheses to explain the particular effect of HS.

Firstly, *a*CXCL12α may be readily released from *i*HS ($K_d \sim 10^{-7}$ M [30, 46]) whereas *i*CXCL12α is quasi-irreversibly attached to the surface *via* strong and stable streptavidin-biotin bonds ($K_d \sim 10^{-14}$ M). Thus, *a*CXCL12α but not *i*CXCL12α may be taken up by the cell, and internalization of CXCL12α has previously been shown to induce downstream signalling [77]. More directly, the transient interaction of CXCL12α with HS may also enable the displacement of the chemokine along the HS matrix after engagement with CXCR4, and thus promote motility by favourably affecting the balance between cell adhesion and detachment.

Secondly, *a*CXCL12α but not *i*CXCL12α is presented together with HS, and a possible explanation therefore is that HS acts as a co-factor of CXCL12α and the two together elicit a different signalling response than the chemokine alone. The role of HS as a co-factor is well established for fibroblast growth factor signalling [78], but to our knowledge has so far not been reported for chemokines. Here, the flexibility and orientational freedom provided by the HS chains may also modulate the recognition of the chemokine by its receptor. The HS film is though too thin to substantially affect the bulk mechanical properties of the substrate, and the surface mechanical properties *per se* are therefore unlikely to modulate myoblast behaviour in a differential way.

Europe PMC Funders Author Manuscripts

Last but not least, CXCL12α is monomeric in solution, and this monomeric state is most likely preserved in the case of *i*CXCL12α given the steric constraints imposed by immobilizing the chemokine through the C-terminal biotin to the streptavidin monolayer. In contrast, HS is known to promote the formation of so-called β-sheet dimers of CXCL12α, by binding to and stabilizing the interface of the two constituent monomers [62, 64, 65]; in addition, we recently suggested that an extended HS matrix may even promote the formation of higher order CXCL12α oligomers [79]. Thus, *a*CXCL12α and *i*CXCL12α are presented in distinct oligomerization states and it is conceivable that myoblasts recognize these differently although we are not aware of such an effect having been reported as of yet and the underlying molecular mechanisms would currently remain obscure.

In principle, one or a combination of any of these effects could account for the distinct ability of HS-bound CXCL12α to facilitate myoblast migration. Future studies that expand on the present approach with additional tailored building blocks such as 'locked' biotinylated dimers or covalently HS-conjugated chemokine, and more readouts such as chemokine internalization or other downstream signalling events will be needed to fully resolve this question.

CXCL12α as the only extrinsic signal is sufficient to promote active cell shape remodelling and migration

In CXCL12α, the binding domain for CXCR4, the binding domain for HS, and the C-terminus are spatially distant and do not interfere functionally [14]. This implies that CXCL12α can interact simultaneously with CXCR4 on one side and HS (*a*CXCL12α) or streptavidin (through the C-terminal biotin, *i*CXCL12α) on another. It is thus not surprising that *a*CXCL12α as well as *i*CXCL12α can promote myoblast attachment even in the absence of cRGD on the biomimetic surfaces (Figs. 2C and H, and S4). It is remarkable, however, that the myoblasts also spread and reduce their circularity following stimulation by *a*CXCL12α or *i*CXCL12α (Fig. 2D-E and I-J), and that they migrate on *a*CXCL12α (Fig. 3), without the extrinsic stimulation of integrins. This implies that CXCL12α as the only extrinsic signal is sufficient to induce active remodelling of the cell shape (which involves actin and also integrins, see above). Moreover, it also suggests that the mechanical link between HS, CXCL12α and CXCR4 can effectively substitute integrins and their extracellular ligands and provide the mechanical traction necessary for cell migration. Future studies should aim to elucidate the intracellular signalling that drives these differential mechanical responses.

We [30] and others [31] have previously shown that engagement with integrin ligands is not required for T lymphocytes to attach to and migrate on chemokine-presenting surfaces. In contrast to myoblasts, T lymphocytes do not adhere to integrin ligands in their naive state and require extrinsic signals such as chemokines and shear stress [31] to activate adhesion *via* integrin receptors. The results presented here thus demonstrate that even for a cell type that does constitutively adhere to integrin ligands, chemokines as the only extrinsic signal are sufficient to promote cell adhesion, active cell shape remodelling and cell migration.

Do integrin ligands potentiate the response of myoblasts towards CXCL12α?

Our results (Figs. 5 and 7) suggest that there is a cooperation between the CXCR4 and integrin receptors in myoblast cells, perhaps similar to the recently demonstrated cooperation between integrins and the receptors of the growth factor bone morphogenetic protein 2 [29]. It is well known that a balanced level of adhesion is required for the optimal migration of cells on integrin-binding substrates (haptotaxis) [80–82]. Previous studies with a constitutively adhesive cell line reported that cell spreading on cRGD presenting surfaces gradually increases as the distance between integrin binding sites approaches 60 nm, and remains constant at distances below 60 nm [83]. In our assays, the mean distance between cRGD ligands is much smaller than this threshold, and a likely reason for the low cell motility on *ld*-*ic*RGD alone (Fig. 7) thus is that adhesion is too strong for optimal migration. Our striking observation that combining *ld*-*a*CXCL12α with *ld*-*ic*RGD simultaneously promoted spreading (Fig. 5) and motility (Fig. 7) to higher levels than those achieved with either of the two ligands alone implies that stimulation with the chemokine effectively overrides the migration blockage and permits high motility along with strong adhesion on integrin-binding substrates. With this finding, we provide novel insight into the effect of chemokines on haptotactic balance, and our methodological approach is ideally suited for further studies in this direction.

Implications for in vivo conditions

Our *in vitro* assays use biomimetic surfaces for which the complexity is greatly reduced compared to the *in vivo* conditions. This is a deliberate choice as the well-defined environment enables the effect of specific parameters on cell behavior to be dissected. These assays provide hypotheses and identify relevant parameters based on which new *in vitro* and *in vivo* assays can be designed to test how cells respond in more complex yet less well defined environments. Questions that require careful consideration, for example, are what the effective dimensionality of myoblast migration [84] is – one dimensional (along defined paths within a fibrillar environment), two dimensional (along cell sheets such as the basal lamina) or three dimensional (across the tissue) – and also whether primary human myoblasts recapitulate the behavior of the popular C2C12 model cell line.

Future application of the developed approach

The platform technology consisting of the glycosaminoglycan HS and the receptor ligands CXCL12α and cRGD may be further used as biomimetic surfaces for mechanistic studies of chemokine-mediated cell-matrix communication and to study the cross-talk between selected chemokine and adhesion surface receptors. Being able to unravel phenotypical changes in response to defined extrinsic signals, the platform may also be used for biological studies of the underlying signal transduction cascades and chemokine signalling pathways. The surface functionalization platform may also be combined with surface patterning, thus enabling studies of the directed migration of cells along a gradient of GAG-bound chemokines.

On a longer term, our results may be used to develop innovative biomaterials for regenerative medicine that are tailored to target chemokine and adhesion receptors in defined ways and thus to promote highly specific cellular responses. CXCL12α is known to be a key

chemokine in a large number of physiological processes, including the homing of hematopoietic stem cells and bone regeneration. cRGD ligands may be used to specifically target cells that could then at the same time be activated by CXCL12α. In this regard, our findings highlight that the mode of CXCL12α presentation is an important parameter to consider in the design of implantable devices delivering CXCL12α to achieve the desired outcome.

5 Conclusion

Using a versatile experimental platform presenting the CXCL12α chemokine and the cRGD integrin ligand, we have shown that the mode of CXCL12α presentation plays an important role in myoblast adhesion and motility. Whereas CXCL12α as the only extrinsic signal is sufficient for myoblast adhesion and spreading, chemokine presentation *via* GAGs is a requisite for myoblast motility. These surfaces mimicking in a very simple way the muscle extracellular matrix provide insights into the role of GAG-bound CXCL12α in muscle development and repair. A cooperative effect was observed when GAG-bound chemokines and integrin ligands were co-presented, which suggests cross-talk between CXCR4 and integrins. Our future studies will aim to study the directed migration of cells on gradients of HS-bound CXCL12α. These multifunctional biomimetic surfaces presenting selected matrix or cell surface components in a well-defined way can be further used for mechanistic studies of chemokine-mediated cell-matrix communication, and may guide the development of tailored biomaterials that promote highly specific cellular responses

Supplementary Material

Refer to Web version on PubMed Central for supplementary material.

Acknowledgements

We gratefully acknowledge Françoise Baleux (Institut Pasteur, Paris, France) for providing b-CXCL12α, Rabia Sadir (Institut de Biologie Structurale, Grenoble, France) for preparing and characterizing recombinant CXCL12α, Luis Yate (CIC biomaGUNE) for surface coatings, and Laure Fourel (Institut Albert Bonniot), Xi Qiu Liu (LMGP) and Jessica C. F. Kwok (University of Leeds) for fruitful discussions. We acknowledge funding by the Nanoscience Foundation Chair of Excellence Project “GAG2D” to RPR, the NanoBio programme, the ICMG FR 2607, and the French National Research Agency *via* Labex ARCANE (ANR-11-LABX-0003-01). CP is grateful to the European Commission for funding *via* an ERC Starting Grant (GA259370).

References

[1]. Yin H, Price F, Rudunicki MA. Satellite cells and the muscle stem cell niche. Physiol Rev. 2013; 93:23–67. [PubMed: 23303905]

[2]. Jansen KM, Pavlath GK. Mannose receptor regulates myoblast motility and muscle growth. J Cell Biol. 2006; 174:403–13. [PubMed: 16864654]

[3]. Thorsteinsdottir S, Deries M, Cachaco AS, Bajanca F. The extracellular matrix dimension of skeletal muscle development. Dev Biol. 2011; 354:191–207. [PubMed: 21420400]

[4]. Mylona E, Jones KA, Mills ST, Pavlath GK. CD44 regulates myoblast migration and differentiation. J Cell Physiol. 2006; 209:314–21. [PubMed: 16906571]

[5]. O’Connor RS, Mills ST, Jones KA, Ho SN, Pavlath GK. A combinatorial role for NFAT5 in both myoblast migration and differentiation during skeletal muscle myogenesis. J Cell Sci. 2006; 120:149–59. [PubMed: 17164296]

[6]. Griffin CA, Apponi LH, Long KK, Pavlath GK. Chemokine expression and control of muscle cell migration during myogenesis. J Cell Sci. 2010; 123:3052–60. [PubMed: 20736301]

[7]. Luster AD. Chemokines - Chemotactic cytokines that mediate inflammation. N Engl J Med. 1998; 338:436–45. [PubMed: 9459648]

[8]. Yusuf F, Rehimi R, Moros¸an-Puopolo G, Dai F, Zhang X, Brand-Saberi B. Inhibitors of CXCR4 Affect the Migration and Fate of CXCR4 Progenitors in the Developing Limb of Chick Embryos. Dev Dyn. 2006; 235:3007–15. [PubMed: 16958136]

[9]. Vasyutina E, Stebler J, Brand-Saberi B, Schulz S, Raz E, Birchmeier C. CXCR4 and Gab1 cooperate to control the development of migrating muscle progenitor cells. Genes Dev. 2005; 19:2187–98. [PubMed: 16166380]

[10]. Odemis V, Lamp E, Pezeshki G, Moepps B, Schilling K, Gierschik P, et al. Mice deficient in the chemokine receptor CXCR4 exhibit impaired limb innervation and myogenesis. Mol Cell Neurosci. 2005; 30:494–505. [PubMed: 16198599]

[11]. Odemis V, Boosmann K, Dieterlen MT, Engele J. The chemokine SDF1 controls multiple steps of myogenesis through atypical PKC. J Cell Sci. 2007; 120:4050–9. [PubMed: 17971416]

[12]. Ratajczak MZ, Majka M, Kucia M, Drukala J, Pietrzkowski Z, Peiper S, et al. Expression of Functional CXCR4 by Muscle Satellite Cells and Secretion of SDF-1 by Muscle-Derived Fibroblasts is Associated with the Presence of Both Muscle Progenitors in Bone Marrow and Hematopoietic Stem/Progenitor Cells in Muscles. Stem Cell. 2003; 21:363–71.

[13]. Melchionna R, Di Carlo A, De Mori R, Cappuzzello C, Barberi L, Musaro A, et al. Induction of myogenic differentiation by SDF-1 via CXCR4 and CXCR7 receptors. Muscle Nerve. 2010; 41:828–35. [PubMed: 20151462]

[14]. Laguri C, Arenzana-Seisdedos F, Lortat-Jacob H. Relationships between glycosaminoglycan and receptor binding sites in chemokines-the CXCL12 example. Carbohydr Res. 2008; 343:2018–23. [PubMed: 18334249]

[15]. Hacker U, Nybakken K, Perrimon N. Heparan sulphate proteoglycans: the sweet side of development. Nat Rev Mol Cell Biol. 2005; 6:530–41. [PubMed: 16072037]

[16]. Sarrazin S, Lamanna WC, Esko JD. Heparan sulfate proteoglycans. Cold Spring Harb Perspect Biol. 2011; 3

[17]. Bernfield M, Gotte M, Park PW, Reizes O, Fitzgerald ML, Lincecum J, et al. Functions of cell surface heparan sukfate proteoglycans. Annu Rev Biochem. 1999; 68:729–77. [PubMed: 10872465]

[18]. Lortat-Jacob H. The molecular basis and functional implications of chemokine interactions with heparan sulphate. Curr Opin Struct Biol. 2009; 19:543–8. [PubMed: 19800217]

[19]. Massena S, Christoffersson G, Hjertstrom E, Zcharia E, Vlodavsky I, Ausmees N, et al. A chemotactic gradient sequestered on endothelial heparan sulfate induces directional intraluminal crawling of neutrophils. Blood. 2010; 116:1924–31. [PubMed: 20530797]

[20]. Rueda P, Balabanian K, Lagane B, Staropoli I, Chow K, Levoye A, et al. The CXCL12gamma chemokine displays unprecedented structural and functional properties that make it a paradigm of chemoattractant proteins. PloS One. 2008; 3:e2543. [PubMed: 18648536]

[21]. Weber M, Hauschild R, Schwarz J, Moussion C, de Vries I, Legler DF, et al. Interstitial dendritic cell guidance by haptotactic chemokine gradients. Science. 2013; 339:328–32. [PubMed: 23329049]

[22]. Monneau Y, Arenzana-Seisdedos F, Lortat-Jacob H. The sweet spot: how GAGs help chemokines guide migrating cells. J Leukoc Biol. 2016; 99:935–53. [PubMed: 26701132]

[23]. Huttenlocher A, Horwitz AR. Integrins in cell migration. Cold Spring Harb Perspect Biol. 2011; 3:a005074. [PubMed: 21885598]

[24]. Hynes RO. The Extracellular Matrix: Not Just Pretty Fibrils. Science. 2009; 326:1216–9. [PubMed: 19965464]

[25]. Mayer U. Integrins: redundant or important players in skeletal muscle? J Biol Chem. 2003; 278:14587–90. [PubMed: 12556453]

[26]. Liu H, Niu A, Chen SE, Li YP. Beta3-integrin mediates satellite cell differentiation in regenerating mouse muscle. FASEB J. 2011; 25:1914–21. [PubMed: 21350117]

[27]. Lan MA, Gersbach CA, Michael KE, Keselowsky BG, Garcia AJ. Myoblast proliferation and differentiation on fibronectin-coated self assembled monolayers presenting different surface chemistries. Biomaterials. 2005; 26:4523–31. [PubMed: 15722121]

[28]. Gribova V, Gauthier-Rouviere C, Albiges-Rizo C, Auzely-Velty R, Picart C. Effect of RGD functionalization and stiffness modulation of polyelectrolyte multilayer films on muscle cell differentiation. Acta Biomater. 2013; 9:6468–80. [PubMed: 23261924]

[29]. Fourel L, Valat A, Faurobert E, Guillot R, Bourrin-Reynard I, Ren K, et al. beta3 integrin-mediated spreading induced by matrix-bound BMP-2 controls Smad signaling in a stiffness-independent manner. J Cell Biol. 2016; 212:693–706. [PubMed: 26953352]

[30]. Migliorini E, Thakar D, Sadir R, Pleiner T, Baleux F, Lortat-Jacob H, et al. Well-defined biomimetic surfaces to characterize glycosaminoglycan-mediated interactions on the molecular, supramolecular and cellular levels. Biomaterials. 2014; 35:8903–15. [PubMed: 25088726]

[31]. Woolf E, Grigorova I, Sagiv A, Grabovsky V, Feigelson SW, Shulman Z, et al. Lymph node chemokines promote sustained T lymphocyte motility without triggering stable integrin adhesiveness in the absence of shear forces. Nat Immunol. 2007; 8:1076–85. [PubMed: 17721537]

[32]. Yoo JW, Irvine DJ, Discher DE, Mitragotri S. Bio-inspired, bioengineered and biomimetic drug delivery carriers. Nature reviews Drug discovery. 2011; 10:521–35. [PubMed: 21720407]

[33]. Rice JJ, Martino MM, De Laporte L, Tortelli F, Briquez PS, Hubbell JA. Engineering the regenerative microenvironment with biomaterials. Advanced healthcare materials. 2013; 2:57–71. [PubMed: 23184739]

[34]. Mehta M, Schmidt-Bleek K, Duda GN, Mooney DJ. Biomaterial delivery of morphogens to mimic the natural healing cascade in bone. Advanced drug delivery reviews. 2012; 64:1257–76. [PubMed: 22626978]

[35]. Cezar CA, Mooney DJ. Biomaterial-based delivery for skeletal muscle repair. Advanced drug delivery reviews. 2015; 84:188–97. [PubMed: 25271446]

[36]. Dalonneau F, Liu XQ, Sadir R, Almodovar J, Mertani HC, Bruckert F, et al. The effect of delivering the chemokine SDF-1alpha in a matrix-bound manner on myogenesis. Biomaterials. 2014; 35:4525–35. [PubMed: 24612919]

[37]. Park S, Gildersleeve JC, Blixt O, Shin I. Carbohydrate microarrays. Chemical Society reviews. 2013; 42:4310–26. [PubMed: 23192235]

[38]. Jonkheijm P, Weinrich D, Schroder H, Niemeyer CM, Waldmann H. Chemical strategies for generating protein biochips. Angew Chem. 2008; 47:9618–47. [PubMed: 19025742]

[39]. Richter RP, Hock KK, Burkhartsmeyer J, Boehm H, Bingen P, Wang G, et al. Membrane-Grafted Hyaluronan Films: A Well-Defined Model System of Glycoconjugate Cell Coats. J Am Chem Soc. 2007; 129:5306–7. [PubMed: 17408270]

[40]. Albertorio F, Daniel S, Cremer PS. Supported Lipopolymer Membranes as Nanoscale Filters: Simultaneous Protein Recognition and Size-Selection Assays. J Am Chem Soc. 2006; 128:7168–9. [PubMed: 16734463]

[41]. Cabanas-Danes J, J H, Jonkheijm P. Chemical strategies for the presentation and delivery of growth factors. J Mater Chem B. 2014; 2:2381–94.

[42]. Mas-Moruno C, Rechenmacher F, Kessler H. Cilengitide: The First Anti-Angiogenic Small Molecule Drug Candidate. Design, Synthesis and Clinical Evaluation. Anticancer Agents Med Chem. 2010; 10:753–68. [PubMed: 21269250]

[43]. Pfaff M, Tangemann K, Muller B, Gurrath M, Muller G, Kessler H, et al. Selective Recognition of Cyclic RGD Peptides of NMR Defined Conformation by aIIbb3, aVb3, and a5bl Integrins. J Biol Chem. 1994; 269:20233–8. [PubMed: 8051114]

[44]. Thakar D, Migliorini E, Coche-Guerente L, Sadir R, Lortat-Jacob H, Boturyn D, et al. A quartz crystal microbalance method to study the terminal functionalization of glycosaminoglycans. Chem Commun. 2014; 50:15148–51.

[45]. Laguri C, Sapay N, Simorre JP, Brutscher B, Imberty A, Gans P, et al. 13C-labeled heparan sulfate analogue as a tool to study protein/heparan sulfate interactions by NMR spectroscopy: application to the CXCL12alpha chemokine. J Am Chem Soc. 2011; 133:9642–5. [PubMed: 21634378]

[46]. Amara A, Lorthioir O, Valenzuel A, Magerus A, Thelen M, Montes M, et al. Stromal Cell-derived Factor-1a Associates with Heparan Sulfates through the First b-Strand of the Chemokine. J Biol Chem. 1999; 274:23916–25. [PubMed: 10446158]

[47]. Boturyn D, Dumy P. A convenient access to aVb3:aVb5 integrin ligand conjugates: regioselective solid-phase functionalisation of an RGD based peptide. Tetrahedron Lett. 2001; 42:2787–90.

[48]. Reviakine I, Johannsmann D, Richter RP. Hearing what you cannot see and visualizing what you hear: interpreting quartz crystal microbalance data from solvated interfaces. Analytical chemistry. 2011; 83:8838–48. [PubMed: 21939220]

[49]. Dubacheva GV, Curk T, Mognetti BM, Auzely-Velty R, Frenkel D, Richter RP. Superselective targeting using multivalent polymers. J Am Chem Soc. 2014; 136:1722–5. [PubMed: 24400591]

[50]. Tumolo T, Angnes L, Baptista MS. Determination of the refractive index increment (dn/dc) of molecule and macromolecule solutions by surface plasmon resonance. Anal Biochem. 2004; 333:273–9. [PubMed: 15450802]

[51]. Pavlov G, Finet S, Tatarenko K, Korneeva E, Ebel C. Conformation of heparin studied with macromolecular hydrodynamic methods and X-ray scattering. Eur Biophys J. 2003; 32:437–49. [PubMed: 12844240]

[52]. Perez Sanchez H, Tatarenko K, Nigen M, Pavlov G, Imberty A, Lortat-Jacob H, et al. Organization of Human Interferon g-Heparin Complexes from Solution Properties and Hydrodynamics. Biochemistry. 2006; 45:13227–38. [PubMed: 17073444]

[53]. Richter, RP., Rodenhausen, KB., Eisele, NB., Schubert, M. Coupling Spectroscopic Ellipsometry and Quartz Crystal Microbalance to Study Organic Films at the Solid-Liquid Interface. Ellipsometry of Functional Organic Surfaces and Films. Hinrichs, K., Eichhorn, K-J., editors. Springer; Heidelberg: 2014. p. 223-48.

[54]. Zhao H, Brown PH, Schuck P. On the distribution of protein refractive index increments. Biophys J. 2011; 100:2309–17. [PubMed: 21539801]

[55]. McMeekin TL, Wilensky M, Groves ML. Refractive indices of proteins in relation to amino acid composition and specific volume. Biochem Biophys Res Commun. 1962; 7:151–6.

[56]. McMeekin, TL., Groves, ML., Hipp, NJ. Refractive indices of amino acids, proteins, and related substances. In Amino Acids and Serum Proteins. Stekol, J., editor. Washington DC: American Chemical Society; 1964.

[57]. Huglin, MB. Specific refractive index increments of polymers in dilute solution. Polymer Handbook. Brandrup, J., Immergut, EH., editors. New York: John Wiley; 1991. p. 409-71.

[58]. Ren K, Fourel L, Rouviere CG, Albiges-Rizo C, Picart C. Manipulation of the adhesive behaviour of skeletal muscle cells on soft and stiff polyelectrolyte multilayers. Acta Biomater. 2010; 6:4238–48. [PubMed: 20601233]

[59]. Plow EF, Haas TA, Zhang L, Loftus J, Smith JW. Ligand binding to integrins. J Biol Chem. 2000; 275:21785–8. [PubMed: 10801897]

[60]. Danhier F, Le Breton A, Preat V. RGD-based strategies to target alpha(v) beta(3) integrin in cancer therapy and diagnosis. Mol Pharm. 2012; 9:2961–73. [PubMed: 22967287]

[61]. Calvete JJ, Fox JW, Agelan A, Niewiarowski S, Marcinkiewicz C. The Presence of the WGD Motif in CC8 Heterodimeric Disintegrin Increases Its Inhibitory Effect on aIIbb3, avb3, and a5b1 Integrins. Biochemistry. 2002; 41:2014–21. [PubMed: 11827548]

[62]. Sadir R, Baleux F, Grosdidier A, Imberty A, Lortat-Jacob H. Characterization of the stromal cell-derived factor-1alpha-heparin complex. J Biol Chem. 2001; 276:8288–96. [PubMed: 11087743]

[63]. Sadir R, Imberty A, Baleux F, Lortat-Jacob H. Heparan sulfate/heparin oligosaccharides protect stromal cell-derived factor-1 (SDF-1)/CXCL12 against proteolysis induced by CD26/dipeptidyl peptidase IV. J Biol Chem. 2004; 279:43854–60. [PubMed: 15292258]

[64]. Fermas S, Gonnet F, Sutton A, Charnaux N, Mulloy B, Du Y, et al. Sulfated oligosaccharides (heparin and fucoidan) binding and dimerization of stromal cell-derived factor-1 (SDF-1/CXCL 12) are coupled as evidenced by affinity CE-MS analysis. Glycobiology. 2008; 18:1054–64. [PubMed: 18796646]

[65]. Murphy JW, Cho Y, Sachpatzidis A, Fan C, Hodsdon ME, Lolis E. Structural and functional basis of CXCL12 (stromal cell-derived factor-1 alpha) binding to heparin. J Biol Chem. 2007; 282:10018–27. [PubMed: 17264079]

[66]. Hunger C, Odemis V, Engele J. Expression and function of the SDF-1 chemokine receptors CXCR4 and CXCR7 during mouse limb muscle development and regeneration. Exp Cell Res. 2012; 318:2178–90. [PubMed: 22766125]

[67]. Juliano RL. Signal transduction by cell adhesion receptors and the cytoskeleton: Functions of Integrins, Cadherins, Selectins, and Immunoglobulin-Superfamily Members. Annu Rev Pharmacol Toxicol. 2002; 42:283–323. [PubMed: 11807174]

[68]. Campbell ID, Humphries MJ. Integrin structure, activation, and interactions. Cold Spring Harb Perspect Biol. 2011; 3

[69]. Kim SH, Turnbull J, Guimond S. Extracellular matrix and cell signalling: the dynamic cooperation of integrin, proteoglycan and growth factor receptor. J Endocrinol. 2011; 209:139–51. [PubMed: 21307119]

[70]. Mattila PK, Lappalainen P. Filopodia: molecular architecture and cellular functions. Nat Rev Mol Cell Biol. 2008; 9:446–54. [PubMed: 18464790]

[71]. Yusuf F, Rehimi R, Morosan-Puopolo G, Dai F, Zhang X, Brand-Saberi B. Inhibitors of CXCR4 affect the migration and fate of CXCR4+ progenitors in the developing limb of chick embryos. Dev Dyn. 2006; 235:3007–15. [PubMed: 16958136]

[72]. Chrzanowska-Wodnicka M, Burridge K. Rho-stimulated Contractility Drives the Formation of Stress Fibers and Focal Adhesions. J Cell Biol. 1996; 133:1403–15. [PubMed: 8682874]

[73]. Pellegrin S, Mellor H. Actin stress fibres. J Cell Sci. 2007; 120:3491–9. [PubMed: 17928305]

[74]. Wozniak MA, Modzelewska K, Kwong L, Keely PJ. Focal adhesion regulation of cell behavior. Biochim Biophys Acta. 2004; 1692:103–19. [PubMed: 15246682]

[75]. Guan JL. Role of focal adhesion kinase in integrin signaling. Int J Biochem Biol. 1997:1085–96.

[76]. Zaidel-Bar R, Cohen M, Addadi L, Geiger B. Hierarchical assembly of cell–matrix adhesion complexes. Biochem Soc Trans. 2004; 32:416–20. [PubMed: 15157150]

[77]. Hatse S, Balzarini J, Liekens S. Stromal cell-derived factor 1 (CXCL12) binds to endothelial cells and signals through a receptor different from CXCR4. Biochem Biophys Res Commun. 2006; 348:192–9. [PubMed: 16875673]

[78]. Ornitz DM, Itoh N. The Fibroblast Growth Factor signaling pathway. Wiley Interdiscip Rev Dev Biol. 2015; 4:215–66. [PubMed: 25772309]

[79]. Migliorini E, Thakar D, Kuhnle J, Sadir R, Dyer DP, Li Y, et al. Cytokines and growth factors cross-link heparan sulfate. Open Biol. 2015; 5:150046. [PubMed: 26269427]

[80]. Huttenlocher A, Ginsberg MH, Horwitz AF. Modulation of cell migration by integrin-mediated cytoskeletal linkages and ligand-binding affinity. J Cell Biol. 1996; 134:1551–62. [PubMed: 8830782]

[81]. Gupton SL, Waterman-Storer CM. Spatiotemporal feedback between actomyosin and focal-adhesion systems optimizes rapid cell migration. Cell. 2006; 125:1361–74. [PubMed: 16814721]

[82]. Dominguez GA, Hammer DA. Effect of adhesion and chemokine presentation on T-lymphocyte haptokinesis. Integr Biol. 2004; 6:862.

[83]. Arnold M, Hirschfeld-Warneken VC, Lohmuller T, Heil P, Blummel J, Cavalcanti-Adam EA, et al. Induction of Cell Polarization and Migration by a Gradient of Nanoscale Variations in Adhesive Ligand Spacing. Nano Lett. 2008; 8:2063–9. [PubMed: 18558788]

[84]. Doyle AD, Wang FW, Matsumoto K, Yamada KM. One-dimensional topography underlies three-dimensional fibrillar cell migration. J Cell Biol. 2009; 184:481–90. [PubMed: 19221195]

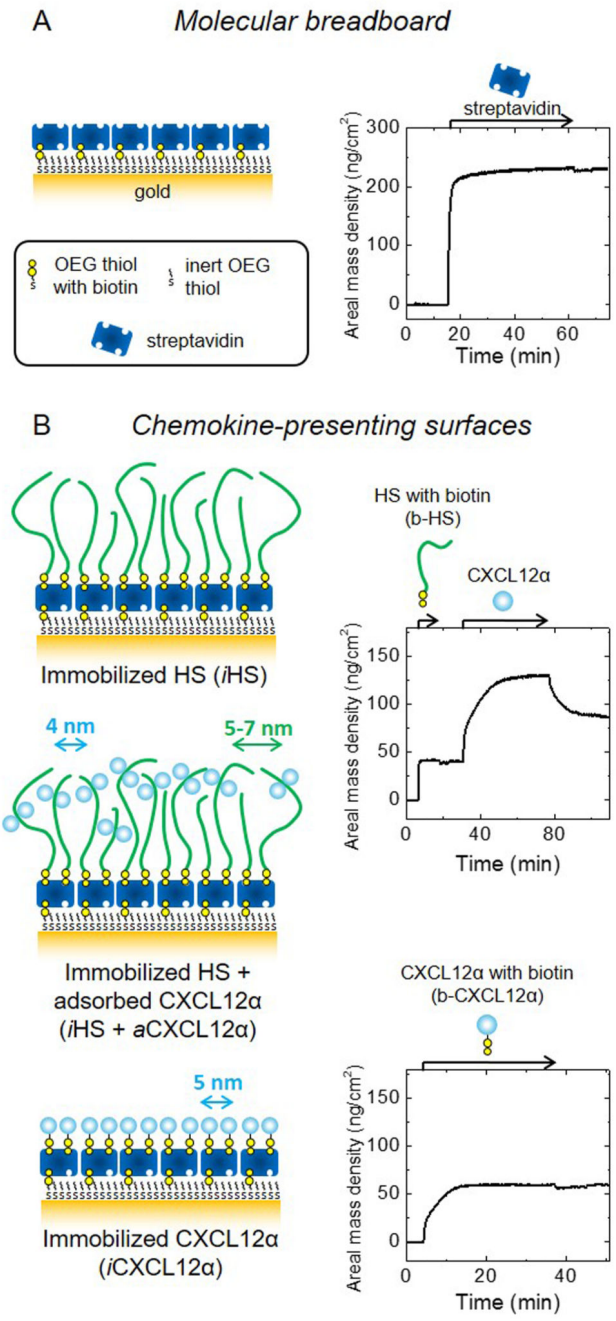

Figure 1. Design and preparation of well-defined biomimetic surfaces presenting GAGs and chemokine.

(A) Schematic presentation of a ‘molecular breadboard’ based on a streptavidin monolayer immobilized on a gold-supported oligoethylene glycol (OEG) monolayer exposing biotin at the end of a fraction of the OEG molecules, where stable attachment to the gold is mediated by thiols. The OEG monolayer (with and without streptavidin) confers a background of low nonspecific binding. (B) Schematic presentation of model surfaces used to study the effect of chemokine presentation on myoblast adhesion and motility: the glycosaminoglycan HS is a native matrix ligand for CXCL12α, and was immobilized (*i*HS) through a biotin at the

reducing end; the chemokine CXCL12α was presented either adsorbed (*a*CXCL12α) through heparan sulfate (HS) or immobilized (*i*CXCL12α) through a C-terminal biotin. All molecules are drawn approximately to scale; arrows indicate the lateral root-mean-square (rms) distance between two molecules (colours of molecules and corresponding arrows are matched); *i*CXCL12α is drawn as monomers but *a*CXCL12α as dimers, reflecting the known propensity of this chemokine to oligomerize upon HS binding. Streptavidin monolayer formation and the functionalization of the molecular breadboard were followed by spectroscopic ellipsometry (SE) to quantify areal mass densities (A and B, right; see also Table 2). Start and duration of incubation steps with different samples are indicated by arrows on top of the SE graphs; during all other times, the surface was exposed to working buffer.

Europe PMC Funders Author Manuscripts

Europe PMC Funders Author Manuscripts

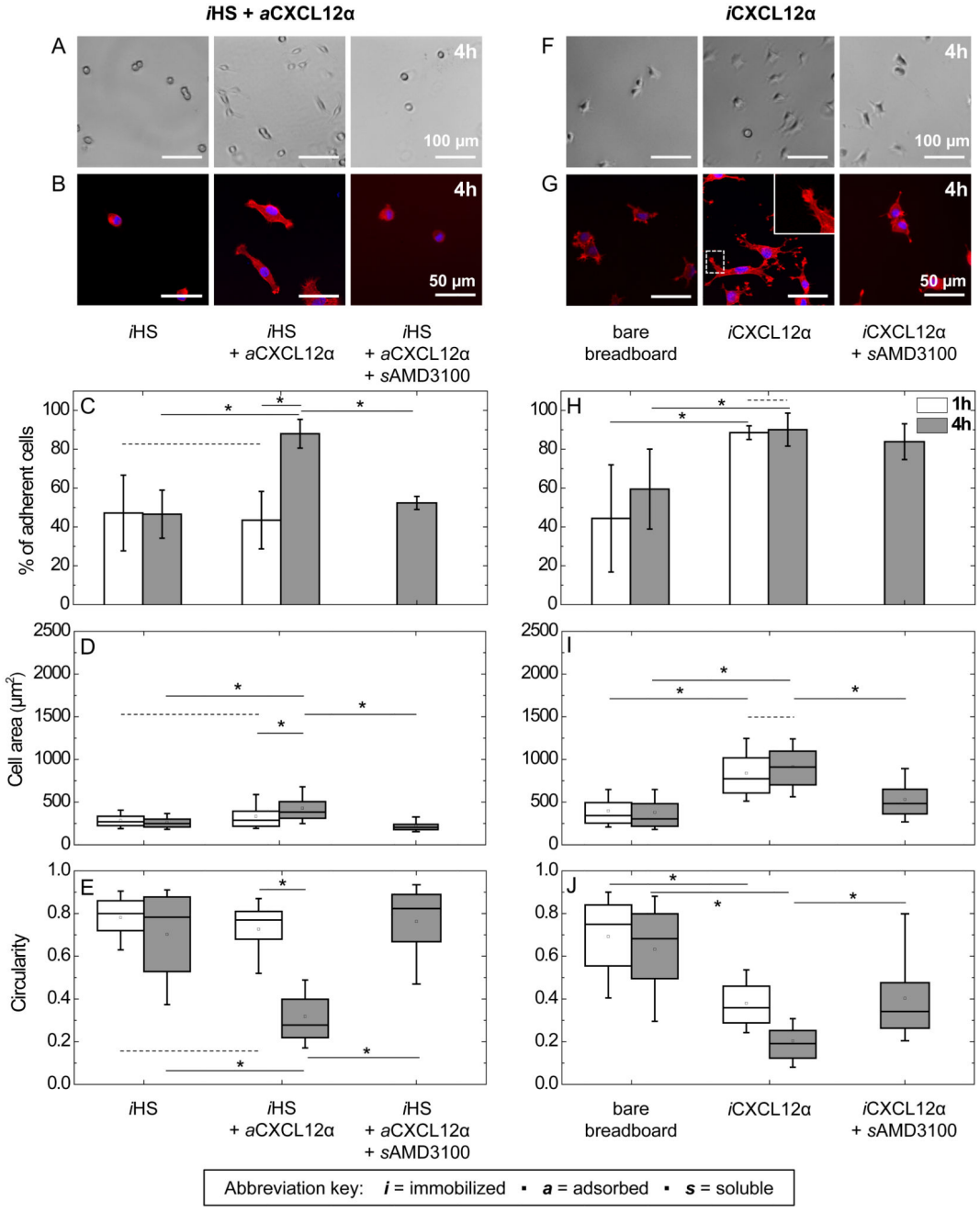

Figure 2. Effect of matrix-bound CXCL12α presentation on C2C12 myoblast adhesion, spreading and circularity.

A to E: adsorbed CXCL12α; F to J: immobilized CXCL12α. Bright-field images of live cells (A and F) and representative fluorescence staining of fixed cells (cell nuclei labeled in blue and actin in red; B and G) for C2C12 myoblasts exposed to surfaces presenting different surface functionalizations for 4 h. The inset in G shows an actin-rich finger-like protrusion at 2× magnification compared to the main image. (C and H) Quantitative analysis of the percentage of adherent cells that remain after gentle rinsing following 1 h (black) and

4 h (blue, hatched) of exposure to different surface functionalizations. The area (D and I) and circularity (E and J) of the adhered cells are displayed as box plots.

Europe PMC Funders Author Manuscripts

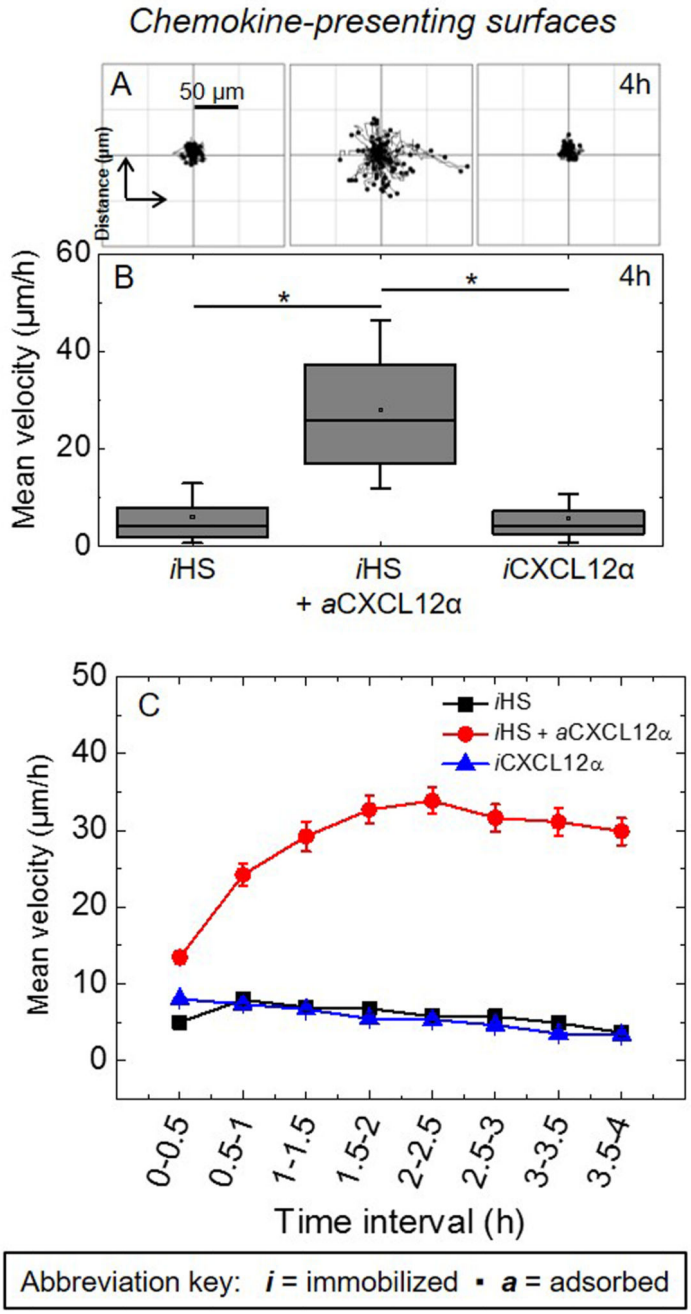

Figure 3. Effect of CXLC12α presentation on cell migration.

(A) Trajectories of the nucleus of C2C12 myoblasts over a period of 4 h after plating on surfaces presenting different surface functionalizations (80 trajectories are shown in each panel, all taken from one representative measurement). (B) Corresponding box plots of the mean velocity (μm/h) throughout 4 h of exposure, computed for a total of 240 cells from three independent measurements. (C) Corresponding variations in the mean velocity as a function of time.

Europe PMC Funders Author Manuscripts

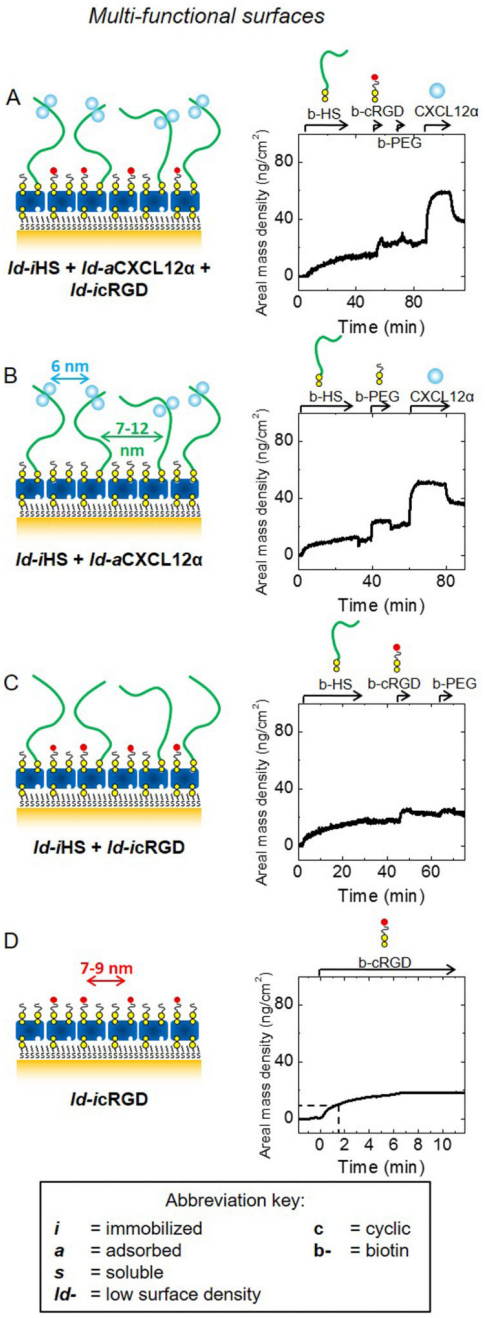

Figure 4. Design and preparation of multifunctional biomimetic surfaces presenting GAG-bound chemokine and integrin ligands.

Schematic presentation of model surfaces (left) used to study the joint effect of HS-bound CXCL12α (*ld-i*HS + *ld-a*CXCL12α) and the immobilized integrin ligand cyclic arginylglycylaspartic acid (*ld-ic*RGD) on myoblast adhesion and motility; surface functionalization was followed by SE to quantify areal mass densities (right; see also Table 2). Schemes and SE data are displayed analogous to Fig. 1B. To accomodate all functional molecules, these were presented at moderately lower densities (*ld*) compared to Fig. 1B; next to surfaces displaying *ld-i*HS, *ld-a*CXCL12α and *ld-ic*RGD (A), controls displaying

only one or two of the three components (B-D) at comparable surface densities were also prepared. cRGD was immobilized through a PEG-linked biotin; biotinylated polyethylene glycol (b-PEG) was used to back-fill the remaining free biotin-binding pockets on the breadboard.

Europe PMC Funders Author Manuscripts

Europe PMC Funders Author Manuscripts

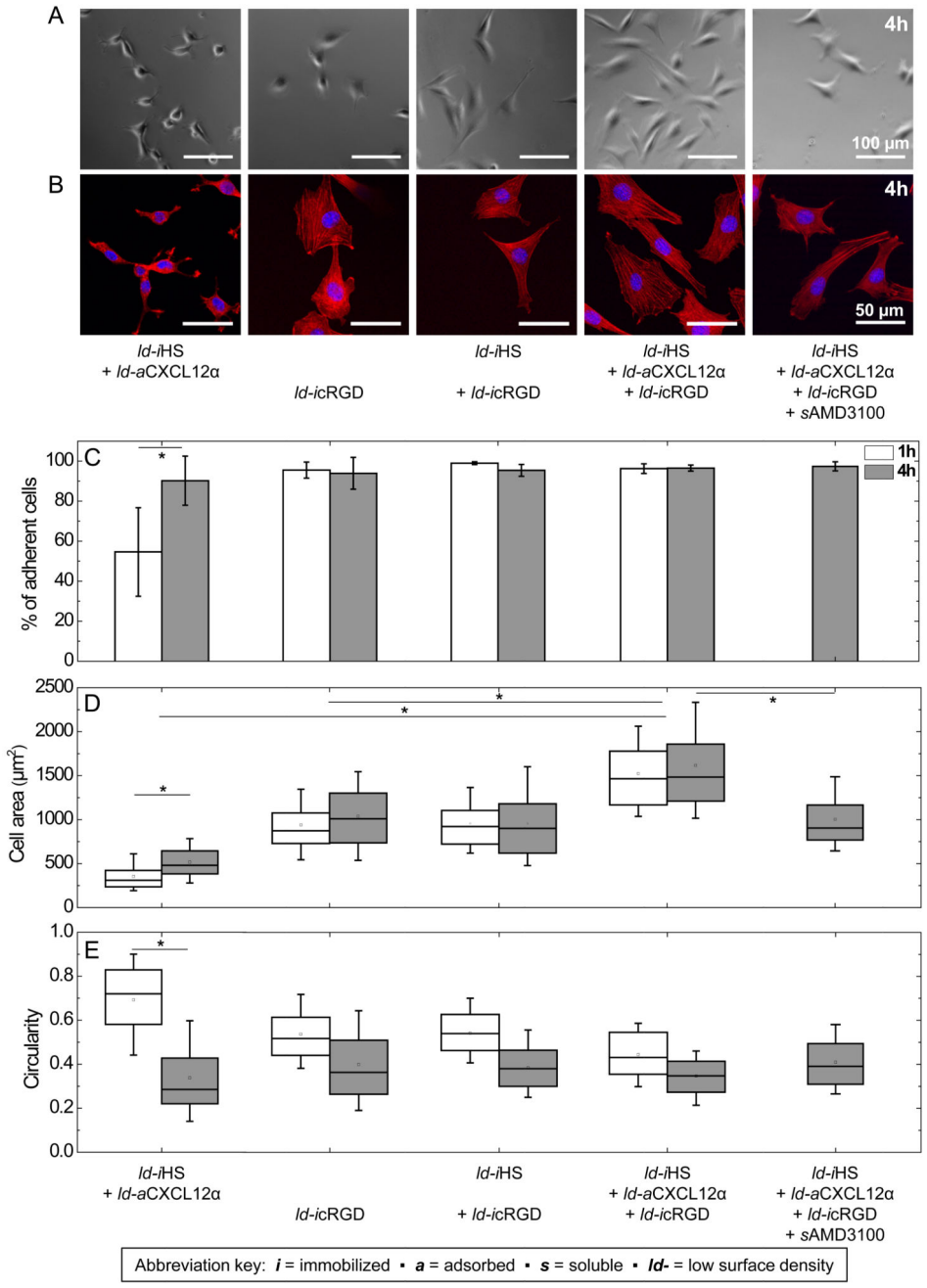

Figure 5. Effect of cRGD, and co-presentation of HS-bound CXCL12α with cRGD, on myoblast adhesion, spreading and circularity.

Adhesion and spreading of C2C12 myoblasts on model surfaces presenting HS (*ld-i*HS) or HS-bound chemokine (*ld-i*HS + *ld-a*CXCL12α) with or without integrin ligand (*ld-ic*RGD), each at comparable surface densities. Data are displayed analogous to Fig. 2.

Europe PMC Funders Author Manuscripts

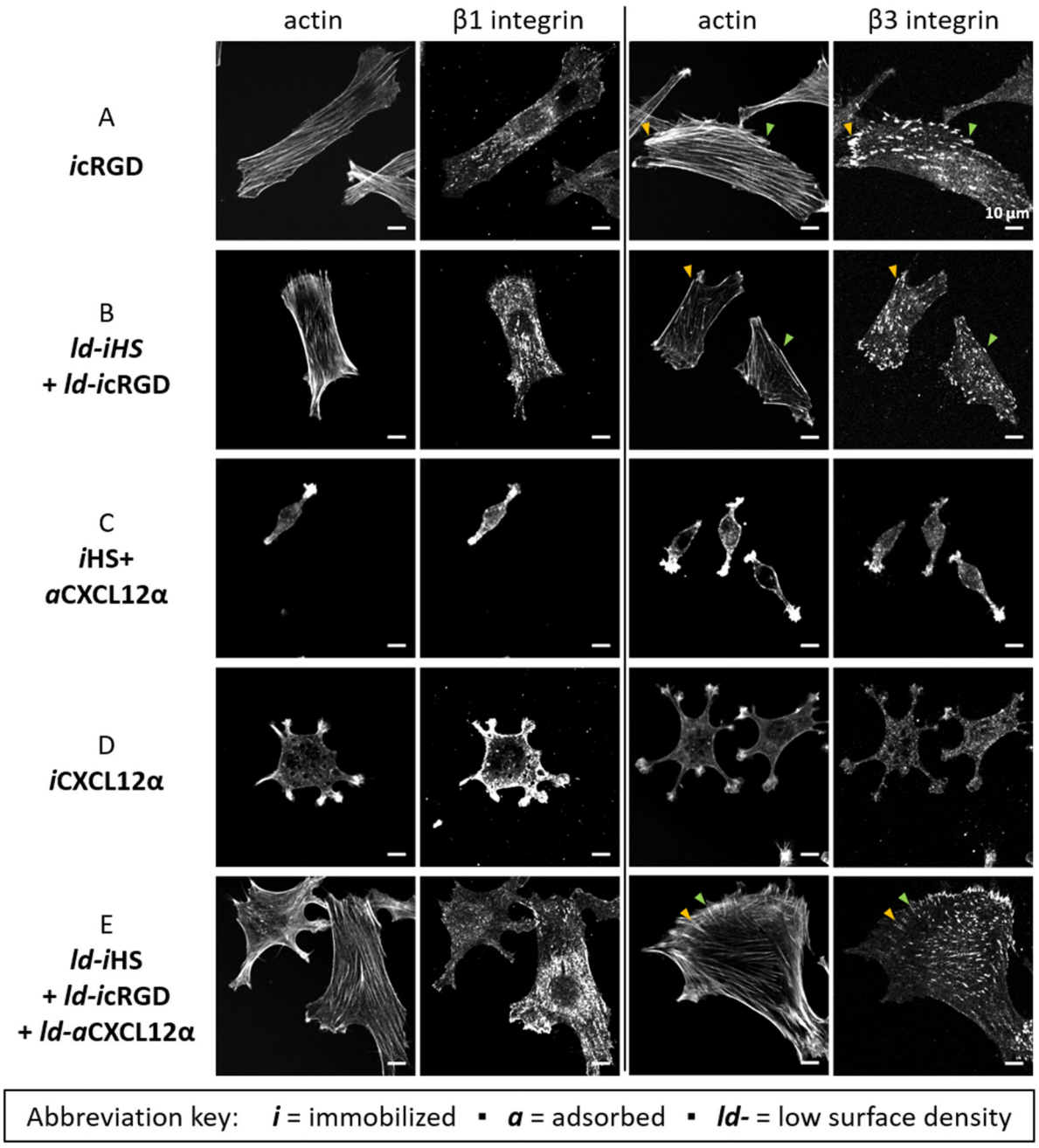

Figure 6. Presence and spatial organization of actin and integrins.

C2C12 myoblasts 4 h post seeding on model surfaces presenting different functionalizations (as indicated on the left) were co-stained for actin and either integrin β_1 or integrin β_3 (as indicated on the top). For optimal contrast perception, this figure is shown in gray scale. Pairs of arrowheads in a given color point to selected β3 integrin-rich puncta (focal adhesions) and the end of their corresponding actin stress fibers.

Europe PMC Funders Author Manuscripts

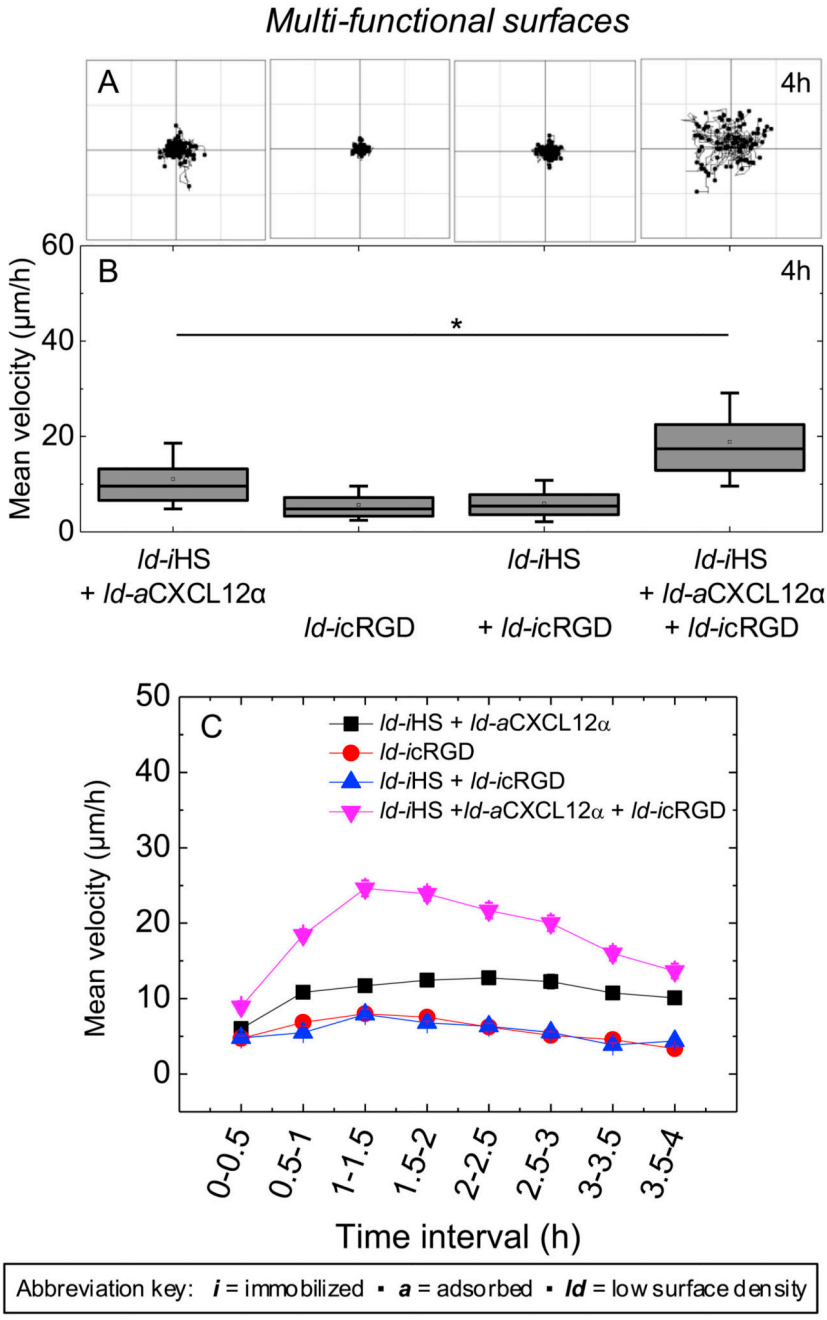

Figure 7. Effect of HS-bound CXLC12α, immobilized cRGD and their combination on cell migration.

(A) Trajectories of the nucleus of C2C12 myoblasts over a period of 4 h after plating on surfaces presenting different surface functionalizations (80 trajectories are shown in each panel, all taken from one representative measurement). (B) Corresponding box plots of the mean velocity (µm/h) throughout 4 h of exposure, computed for a total of 240 cells from three independent measurements. (C) Corresponding variations in the mean velocity as a function of time.

Europe PMC Funders Author Manuscripts

Table 1

Prefixes used to indicate modes of molecule presentation, and molecular properties and tags.

Prefix	Meaning	Used as			
		Mode of molecule presentation			
a	**a**dsorbed		*a*CXCL12α		
i	**i**mmobilized	*i*HS,	*i*CXCL12α,	*ic*RGD	
s	**s**oluble		*s*CXCL12α,	*sc*RGD,	*s*AMD3100
ld-	**l**ow surface **d**ensity	*ld-i*HS,	*ld-a*CXCL12α,	*ld-ic*RGD	
		Molecular properties and tags			
c	**c**yclic			cRGD	
b-	**bi**otinylated	b-HS,	b-CXCL12α,	b-cRGD,	b-PEG

Table 2

Adsorbed amounts (Γ) and root-mean-square anchor distances r_{rms} for the constituents of biomimetic surfaces.

Data were extracted from SE measurements. Mean values and standard errors are presented.

	b-HS		CXCL12α		b-CXCL12α		b-cRGD	
	Γ (ng/cm^2)	r_{rms} (nm)	Γ (ng/cm^2)	r_{rms} (nm)	Γ (ng/cm^2)	r_{rms} (nm)	Γ (ng/cm^2)	r_{rms} (nm)
Chemokine-presenting surfaces								
*i*HS + *a*CXCL12α	40 ± 2	5 - 7[a)]	78 ± 7	4.1 ±0.2				
*i*CXCL12α					60 ± 1	4.9 ±0.1		
Multi-functional surfaces								
*ld-i*HS + *ld-a*CXCL12α + *ld-i*cRGD[b)]	15 ± 1	7 - 12[a)]	37 ± 3	6.0 ±0.3			9 ± 2	7 - 9[a)]

[a)] Upper bounds are determined by assuming that the average molecular mass of surface-bound molecules is identical to the average solution-phase molecular mass; lower bounds are determined assuming a stoichiometry of two biotinylated molecules per streptavidin at maximal coverage.

[b)] All the controls, *i.e.* surfaces that lacked one or two of the biofunctional components (HS, CXCL12α, or cRGD) present all remaining biofunctional components with surface densities and rms distances unchanged.